Non-Linear Signature in Ultrasonic Pulse-Echo Signal for Structural Health Monitoring of Fatigue Induced Composite Structures

HOSSAIN AHMED, ASEF ISHRAQ SADAF
and SOURAV BANERJEE

ABSTRACT

Experimental evaluation of material state damage due to frequency varied fatigue loading has been reported in this article by estimating the non-linearity in ultrasonic signals in CFRP composite structures. In recent years, researchers have been utilizing the non-linearity in Lamb wave propagation for structural health monitoring, and thus it is becoming a powerful technique for non-destructive evaluation. Unlike isotropic and homogeneous materials, the damage state modeling of composite structures is complex due to their heterogeneous arrangement of material constituents, especially in fatigue induced loading cycles. Although established for metals and alloys, the quantification of material state of carbon fiber reinforced viscoelastic polymer composites due to dynamic loading environment is still under an active research area. This research evaluates the non-linearity effect in stress relaxation using high frequency (~25 MHz) ultrasonic pulse-echo signals. A set of tensile test specimen as per ASTM standard is prepared and fatigue loads are applied at constant time intervals. During these intervals, scanning acoustic microscope is used to generate and capture pulse-echo signals. The change of second and third order non-linearity parameter of ultrasonic pressure waves are correlated with the fatigue induced internal stresses and damage accumulations. Initial investigation indicates that the higher order non-linearity is a function of applied fatigue loading frequency and the remaining life of the composite structure.

INTRODUCTION

The existence of non-linearity effect in ultrasonic Lamb wave propagation has been a well-established phenomenon in recent years [1, 2]. The non-linearity effect in wave propagation has been utilized to monitor structural health, more specifically this technique is well suited for material state assessment, precursor damage estimation and

Hossain Ahmed, Department of Mechanical Engineering, Georgia Southern University, Statesboro, GA 30458
Asef Ishraq Sadaf, Department of Mechanical Engineering, Georgia Southern University, Statesboro, GA 30458
Sourav Banerjee, Department of Mechanical Engineering, University of South Carolina, Columbia, S C 29201

remaining strength prediction of composite structures [3, 4]. While the application of linear Lamb waves is limited to the inspection of discrete damage such as delamination and open crack, the multi-advantages of the guided wave over the bulk waves provides stark attention to the application of non-linear properties of Lamb waves. In this perspective, the research on the non-linearity effect in pressure wave propagation in solids is yet to be explored and a growing field with immense potentiality [5, 6]. Ultrasonic assessment of composite structures largely utilizes pressure wave for material state estimation [7, 8]. Without understanding nonlinear properties of bulk wave propagation, composite structure assessment can be considered incomplete. To address this gap and to explore the potential application of non-linearity in pressure wave propagation, in this study, the existence and the estimation of non-linearity in high frequency ultrasonic acoustic pressure propagation is reported. The theoretical foundation of acoustic non-linearity is described in the following paragraphs. 1-D wave equation in x-direction can be written as,

$$\rho \frac{\partial^2 u}{\partial t^2} = \frac{\partial \sigma_{xx}}{\partial x} \tag{1}$$

Constitutive equation for non-linear materials in 1-D can be written as [9],

$$\sigma_{xx} = E_{xx}\varepsilon_{xx}(1 + \beta\varepsilon_{xx} + \gamma(\varepsilon_{xx})^2 + \ldots\ldots) \tag{2}$$

Where $\boldsymbol{\sigma_{xx}}$, $\boldsymbol{\varepsilon_{xx}}$ and $\boldsymbol{E_{xx}}$ are stress in the x-direction, strain in the x-direction, Young's modulus. $\boldsymbol{\beta}$ and γ are second and third order nonlinearity parameter, respectively. By substituting equation (2) in equation (1), we can write the equation of motion including the second and third order non-linearity as [10],

$$\rho \frac{\partial^2 u}{\partial t^2} = E_{xx}\frac{\partial^2 u}{\partial x^2} + \beta E_{xx}\frac{\partial u}{\partial x}\frac{\partial^2 u}{\partial x^2} + \gamma E_{xx}\frac{\partial^2 u}{\partial x^2}\left[\frac{\partial u}{\partial x}\right]^2 \tag{3}$$

The classical solution of displacement parameter u can be obtained by applying perturbation theory and hence u can be written as,

$$u = A_1 \cos(kx - \omega t) - A_2 \sin 2(kx - \omega t) \tag{4}$$

Absolute second and third order non-linearity parameter can be expressed as [11],

$$\beta = \frac{8}{k^2 x} \cdot \frac{A_2}{A_1^2} \cdot f(\omega) \tag{5}$$

$$\gamma = \frac{32}{k^4 x^2} \cdot \frac{A_3}{A_1^3} \cdot f(\omega) \tag{6}$$

In equation (5) and (6), the amplitude of the fundamental, second and third harmonics are denoted by A_1, A_2 and A_3. The propagation distance, wavenumber and a frequency function are defined by x, k and $f(\omega)$ respectively. The normalized second and third order non-linearity, $\tilde{\beta}$ and $\tilde{\gamma}$, can be expressed as [12],

$$\tilde{\beta} = \frac{A_2}{A_1^2} \propto \beta x \tag{7}$$

$$\tilde{\gamma} = \frac{A_3}{A_1^3} \propto \gamma x^2 \quad (8)$$

EXPERIMENTAL INVESTIGATION

The focus of this experimental study is to induce repetitive mechanical fatigue load to a woven composite structural material with a constant interval so that the non-linearity effect of induced stresses can be observed. First, woven composite specimens are prepared according to ASTM 3039 standard from commercially available four layer woven composite panels. Each layer of the fabric is weaved with 3k carbon fiber tows in [0, 90] direction. The density of the specimens is reported by the vendor as 1605 kg/m^3. In total 9 specimens are prepared with final dimensions of 250mm (L), 25 mm (W) and 1.5 mm (T). 6 out of 9 specimens are reserved for tensile-tensile fatigue testing followed by investigations with Scanning Acoustic Microscope (SAM) to estimate material properties. The remaining 3 specimens are utilized to verify the stress-strain properties of the prepared composite plate samples [6, 7]. These three specimens are tested under incremental tensile load to establish the stress-strain behavior of the woven composites. The average ultimate strength is found to be ~8,400 lbf.

Fatigue Testing Parameters

As stated in Figure 1(b), two fatigue loading rates, 2 Hz and 5 Hz, are employed for tensile-tensile fatigue investigations. More specifically, three specimens are reserved for 2 Hz fatigue load and the other three specimens are reserved for 5 Hz fatigue loading rate. An MTS 820 machine is utilized to perform tensile-tensile fatigue testing. In this study, the fatigue loading ratio, ${}^{\sigma_{min}}/_{\sigma_{max}}$ is determined as 0.01 where σ_{max} is 60% of the σ_{ult} [2]. For each loading rate, after completion of each 75,000 fatigue cycles (see Figure 1a), each specimen is kept under water without any loading at room temperature for 8 hours for stress relaxation.

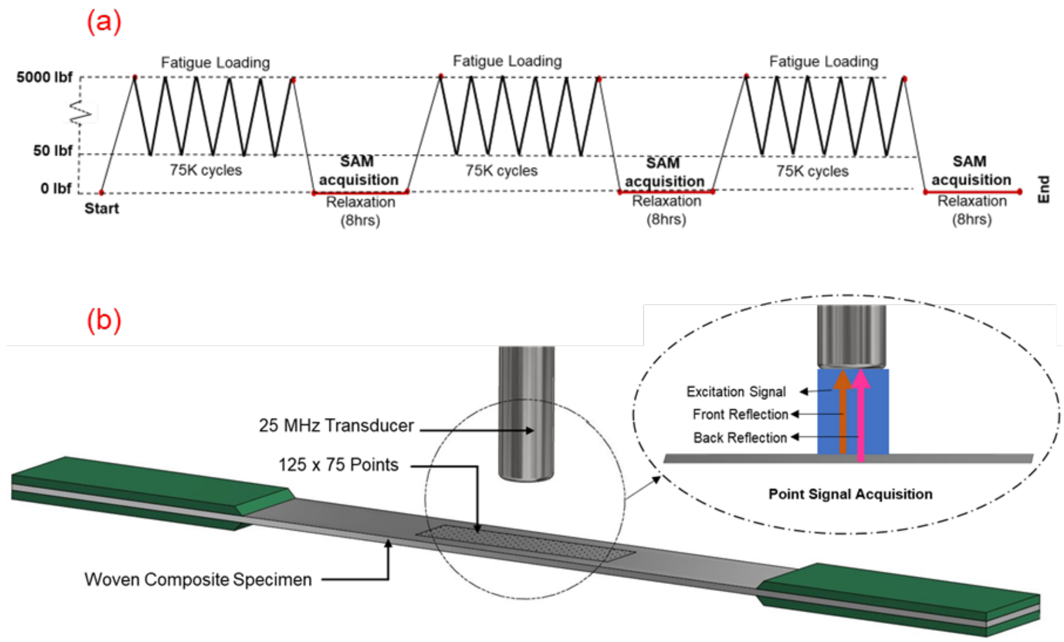

Figure 1: (a) Design of three stages of fatigue testing and 8-hour relaxation experiment. (b) Pulse-Echo data acquisition using scanning acoustic microscope

Scanning Acoustic Microscopy

As stated in Figure 1(a), after completion of each 75000 fatigue cycles at a specified loading rate, the specimens are placed under 50 mm of distilled water at room temperature. Ultrasonic scanning is performed while the specimens are inside the water. While the specimens are kept without loading (which is named as stress relaxation period), the scanning procedure is started by exciting the ultrasonic p-wave. This is done by means of a 25 MHz transducer mounted ~35 mm above the test specimen. The generated signals pass through the water and form a focal region on the top surface of the specimen. Once the acoustic wave interacts with the top surface, some part of the wave energy reflects back to the transducer and the rest of the energy goes through the specimen (through thickness direction). Once the wave energy interacts with the bottom surface of the specimen, it reflects again back to the transducer. The signals reflected from the top surface (water-composite interphase) and the bottom surface (composite-water interphase) are received by the actuating transducer. The time difference between these two reflections is the time of flight which is captured by the SAM [13, 14]. The signals received from a point on the composite specimen are averaged from 10,000 samples to minimize the noise effect. An area at the mid-section of the specimen is chosen and the signals from 125 × 75 points distributed in x-y plane are collected at each trial. This process is repeated at an interval of 15-minutes for 8 hours.

RESULTS AND DISCUSSION

As illustrated in Figure 1(b), the time domain signals are collected during the stress relaxation period, and these signals are analyzed for non-linearity parameters. As the fatigue loading rates and the cycles increase, the micro-damage, in terms of micro-cracks, is prone to increase. Understanding the effect of fatigue loading rate and subsequent fatigue cycles on the composite damage state requires the transformation of the time-domain signal into a frequency-domain signal. Moreover, it is evident, from Eqs. X to Y, the acoustic non-linearity is a function of frequency and signal amplitudes. Therefore, Fast Fourier Transformation (FFT) is performed on the time-domain signals acquired from 125×75 points on each specimen. The frequency of the maximum amplitude in the transformed frequency domain signal is known as the first harmonic frequency. The second and third harmonic frequencies are two and three times of the first harmonic frequency. In this study, all these three frequencies are extracted from the frequency domain signals. Since a large set of first harmonic frequencies are obtained from the time domain signals of 125×75 points at the beginning of the first stage relaxation, a statistical probability distribution is used to determine the mean value of the first harmonic frequency at any instance. In this study, utilizing the frequency domain data, a normal distribution is fitted. Afterwards, the mean value and the standard deviation of the first harmonic frequency are obtained. Since SAM data is captured in every 15 minutes interval, 32 data points are obtained in 8-hour relaxation periods. In Figure X, the mean values and one-tenth of the standard deviation ($\mu \pm 0.1\sigma$) of the first harmonic frequency are plotted for the first, second and third stage relaxation periods. It can be noted that these chronological representations of the first harmonic frequencies are obtained after each 75,000 fatigue cycles. A trend line is plotted that passes through the mean values of the first harmonic frequencies (middle line in each relaxation stage). From Figure 2, for 2 Hz fatigue loading rate, the mean values of the

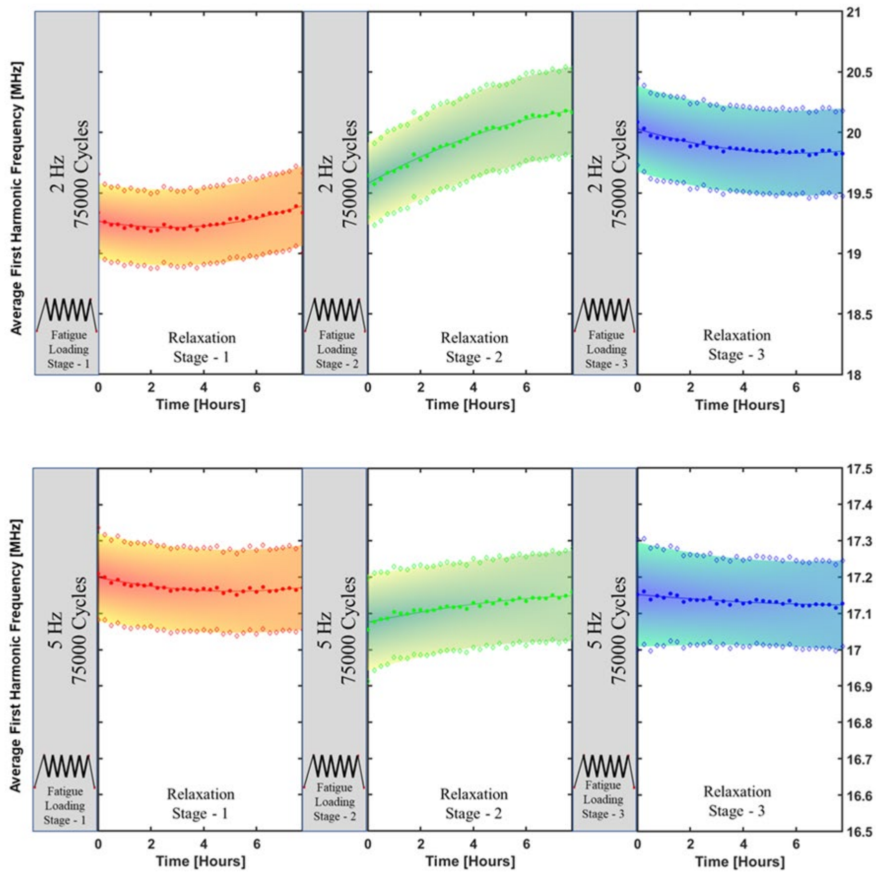

Figure 2: Plot of $\mu \pm 0.1\sigma$ of first harmonic frequencies over 8-hour relaxations period for 2 Hz (top) and 5 Hz (bottom) fatigue loaded specimen.

first harmonic frequencies increases throughout the first stage relaxation, however, in the second stage of relaxation, this increment of the mean value is higher than the first stage relaxation. In the third stage relaxation, these values seem stabilized. On the other hand, for 5 Hz fatigue loading rate, during the first stage and third stage relaxations, the mean values decreased over the relaxation period whereas during the second stage relaxation period, the mean values increased. In comparison of 2 Hz and 5 Hz data, it is evident that the mean values and the range mean values of first harmonic frequencies in 2 Hz is higher than that of 5 Hz data. The decrease in mean values of first harmonic frequencies indicates the formation of damage such as micro-crack, delamination, or any other form of irregularities inside the composite structure due to the increment of fatigue loading rate.

Figure 3 shows the second order non-linearity which is defined by $\tilde{\beta}$ (see equation 7) for specimens that go through the 2 Hz and 5 Hz fatigue loading rate. It can be noted that the $\mu \pm 0.1\sigma$ of the $\tilde{\beta}$ values are plotted chronologically in each relaxation stages. In these representations, it is evident that, for 2 Hz fatigue loaded specimens, the second order non-linearity increases during first stage relaxation whereas it decreases during the second stage relaxation. In the third stage relaxation, it increases slightly. For

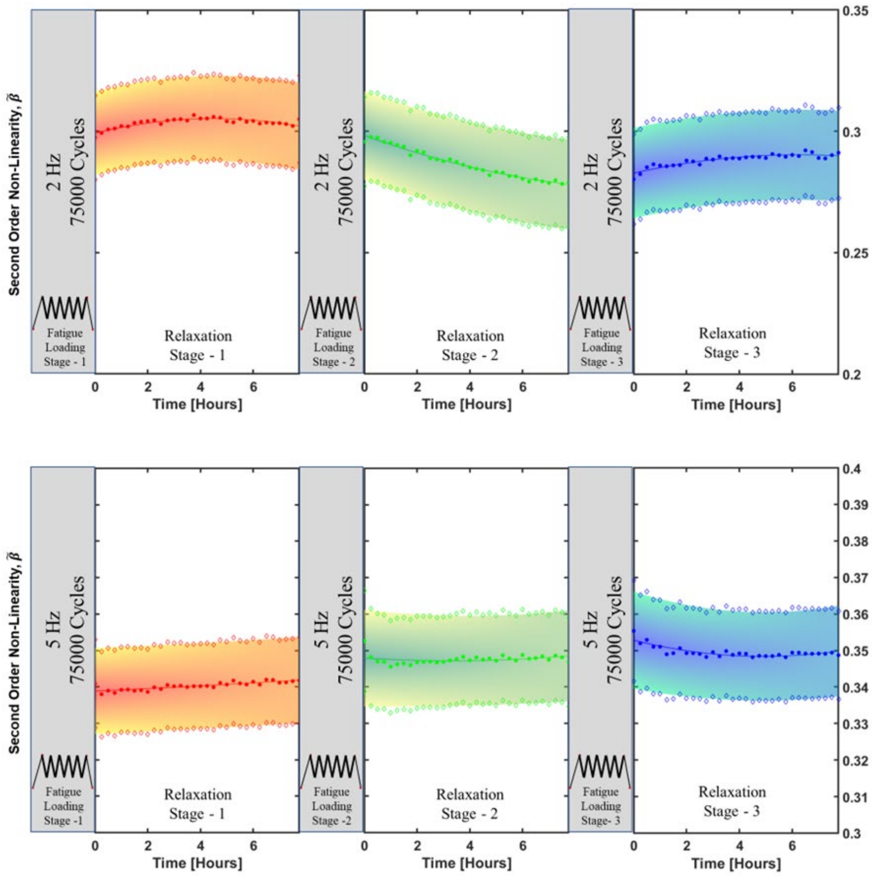

Figure 3: Plot of $\mu \pm 0.1\sigma$ of second order nonlinearity, $\tilde{\beta}$, over 8-hour relaxations period for 2 Hz (top) and 5 Hz (bottom) fatigue loaded specimen.

5 Hz fatigue loaded specimens, the second order nonlinearity increases during all three relaxation stages. In comparison of 2 Hz and 5 Hz specimens, the second order nonlinearity parameter in 5 Hz fatigue loaded specimens are higher than the 2 Hz fatigue loaded specimens. This indicates that as the fatigue loading rate increases, the values of $\tilde{\beta}$ also increases. As mentioned earlier, increased fatigue loading rate induces damage in the form of micro-crack, delamination or any other forms. Therefore, the increment of $\tilde{\beta}$ is an indicative of damage induced in a composite structure.

Figure 4 shows the third order non-linearity which is defined by $\tilde{\gamma}$ (see equation 8) for specimens that go through the 2 Hz and 5 Hz fatigue loading rate. It can be noted that the $\mu \pm 0.1\sigma$ of the $\tilde{\gamma}$ values are plotted chronologically in each relaxation stages. In these representations, it is evident that specimen with 2 Hz fatigue loading rate the third order nonlinearity increases slightly in first and second stage relaxation. Over second stage relaxation, $\tilde{\gamma}$ value decreases slightly. For 5 Hz fatigue loaded specimens, the increase of $\tilde{\gamma}$ over the first relaxation period is clearly evident whereas a significant shift in $\tilde{\gamma}$ values is seen in second stage relaxation. The trend in $\tilde{\gamma}$ values in second and third stage relaxation is seen slightly decreasing over these two relaxation periods. Since

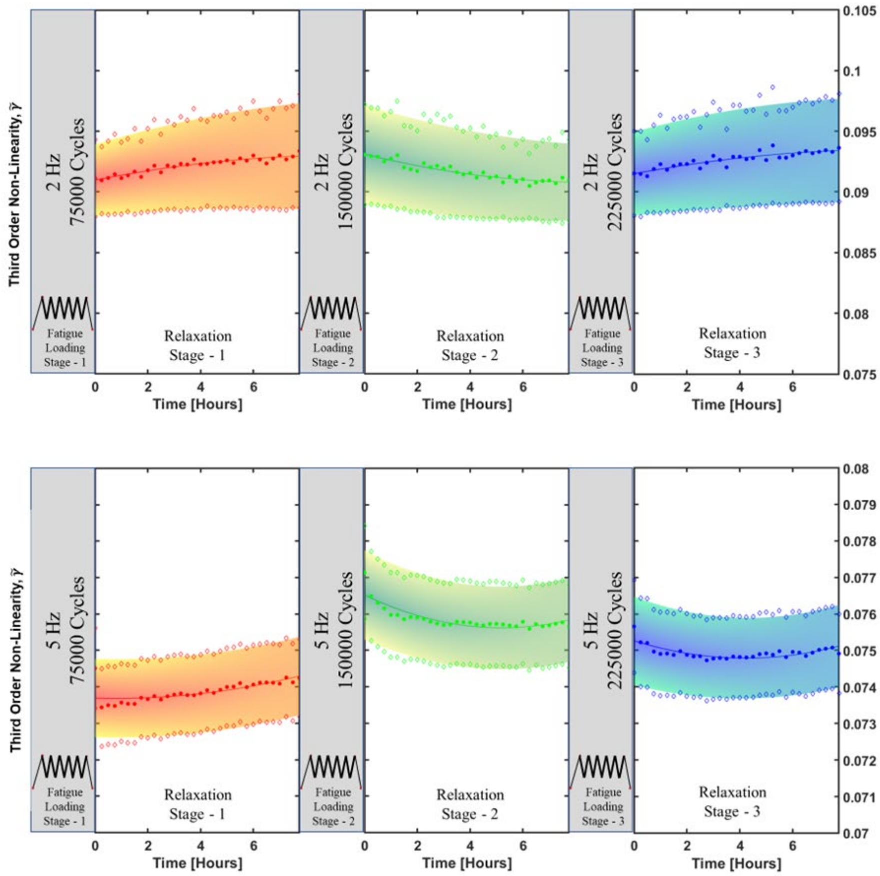

Figure 4: Plot of $\mu \pm 0.1\sigma$ of third order nonlinearity, $\tilde{\gamma}$, over 8-hour relaxations period for 2 Hz (top) and 5 Hz (bottom) fatigue loaded specimen.

the third order non-linearity can be explained by equation 8, the absolute amplitude of the third harmonic frequency is relatively small. Therefore, the values of $\tilde{\gamma}$ is one order less than $\tilde{\beta}$. In comparison of $\tilde{\gamma}$ for both 2 Hz and 5 Hz specimens, $\tilde{\gamma}$ of 2 Hz specimens are less than that of 5 Hz specimens which shows an opposite trend compared to $\tilde{\beta}$. This can be explained by the fact that specimens that go through the 5 Hz fatigue frequency loading rate, incurs micro-damages for which the amplitude of the third harmonic frequency is smaller than that of 2 Hz frequency and thus $\tilde{\gamma}$ values are highly sensitive to the fatigue loading rate.

CONCLUSION

In this study, a non-linearity analysis on high frequency ultrasonic pulse-echo signals is performed for fatigue loaded CFRP-woven composite structures. The ASTM standard test specimens are prepared from composite panel and tensile-tensile fatigue loads are applied to these specimens in two categories of loading rate, 2 Hz and 5 Hz. Three stages of fatigue loading cycles followed by a relaxation period are allowed for the specimens. After completion of each 75000 cycles, specimens are kept in room temperature water where Scanning Acoustic Microscopy is performed. The time domain signals acquired by the SAM are transformed into frequency domain signals, and the second and third order nonlinearity parameters are estimated over the three stages of relaxation periods. From these nonlinearity parameters, it is evident that the specimens that go through the 5 Hz fatigue loading rate, the second order nonlinearity increases chronologically over the relaxation periods whereas the specimens that go through the 2 Hz fatigue loading rate show an incremental third order nonlinearity in each stage of relaxation. Therefore, the nonlinearity parameter can be an indication of material degradation in composite structures.

REFERENCES

1. Patra, S., H. Ahmed, M. Saadatzi, and S. Banerjee, Evidence of dissipative and growing nonlinearity in Lamb waves due to stress-relaxation and material degradation in composites. Ultrasonics, 2019. 96: p. 224-231.
2. Patra, S., H. Ahmed, M. Saadatzi, and S. Banerjee, Effect of Time-Dependent Strength Recovery of Composite Materials: Quantification Through Higher Order Ultrasonic Non-Linearity Using Lamb Waves. Journal of Nondestructive Evaluation, Diagnostics and Prognostics of Engineering Systems, 2019. 3(1).
3. Chen, H., M. Liu, Y. Chen, S. Li, and Y. Miao, Nonlinear Lamb Wave for Structural Incipient Defect Detection with Sequential Probabilistic Ratio Test. Security and Communication Networks, 2022. 2022: p. 9851533.
4. Li, X., G. Shui, Y. Zhao, and Y.-S. Wang Propagation of Non-Linear Lamb Waves in Adhesive Joint with Micro-Cracks Distributing Randomly. Applied Sciences, 2020. 10, DOI: 10.3390/app10030741.
5. Kewalramani, J.A., Z. Zou, R.W. Marsh, B.G. Bukiet, and J.N. Meegoda Nonlinear Behavior of High-Intensity Ultrasound Propagation in an Ideal Fluid. Acoustics, 2020. 2, 147-163 DOI: 10.3390/acoustics2010011.
6. Iqbal, A., M.J. Siddiqui, I. Muhi, M. Abbas, and T. Akram, Nonlinear waves propagation and stability analysis for planar waves at far field using quintic B-spline collocation method. Alexandria Engineering Journal, 2020. 59(4): p. 2695-2703.
7. Obaid, N., M.T. Kortschot, and M. Sain, Predicting the stress relaxation behavior of glass-fiber reinforced polypropylene composites. Composites Science and Technology, 2018. 161: p. 85-91.
8. Hossain Ahmed, M.S., Subir Patra, Sourav Banerjee. Entropy-Based Damage Evaluation of Composite Structure and Its Application to Structural Health Management. in Structural health monitoring. 2019. CA, USA.
9. Shen, Y. and V. Giurgiutiu, Predictive modeling of nonlinear wave propagation for structural health monitoring with piezoelectric wafer active sensors. Journal of Intelligent Material Systems and Structures, 2014. 25(4): p. 506-520.
10. Shen, Y. and V. Giurgiutiu, Predictive modeling of nonlinear wave propagation for structural health monitoring with piezoelectric wafer active sensors. Journal of Intelligent Material Systems and Structures, 2013. 25(4): p. 506-520.
11. Gebrekidan, S.B., T. Kang, H.J. Kim, and S.J. Song, Nonlinear ultrasonic characterization of early degradation of fatigued Al6061-T6 with harmonic generation technique. Ultrasonics, 2018. 85: p. 23-30.
12. Li, W., Y. Cho, and J.D. Achenbach, Detection of thermal fatigue in composites by second harmonic Lamb waves. Smart Materials and Structures, 2012. 21(8): p. 085019.
13. Saadatzi, M., H. Ahmed, S. Patra, and S. Banerjee. Utilization of Scanning Acoustic Microscope (SAM) to prove the existence of stress relaxation in woven composite. in Smart Structures and NDE for Energy Systems and Industry 4.0. 2019.
14. Mohammad Sadegh, S., A. Hossain, I. Mustahseen Mobashwer, and B. Sourav. RUSH: Realtime ultrasonic scanning using submergible hydraulic robotic arms for mechanical properties testing. in Proc.SPIE. 2019.